

Photoresponsive properties at (001), (111) and (110) LaAlO₃/SrTiO₃ interfaces

Hong Yan¹, Zhaoting Zhang¹, Ming Li¹, Shuanhu Wang¹, Lixia Ren¹ and Kexin Jin¹

Shaanxi Key Laboratory of Condensed Matter Structures and Properties and MOE Key Laboratory of Materials Physics and Chemistry under Extraordinary Conditions, School of Science, Northwestern Polytechnical University, Xi'an 710072, People's Republic of China

E-mail: jinkx@nwpu.edu.cn

Received 30 June 2019, revised 20 November 2019

Accepted for publication 4 December 2019

Published 31 December 2019



Abstract

We report the photoresponsive characteristics of (001), (110), and (111) LaAlO₃/SrTiO₃ heterointerfaces deposited at different oxygen pressures using a 360 nm light. The results show that LaAlO₃/SrTiO₃ interfaces with less oxygen vacancies exhibit a larger resistance change when illuminated by light and a slower recovery process when light is off. In addition, the (110) LaAlO₃/SrTiO₃ heterointerfaces present the smallest photoinduced change and residual photoinduced change in the resistance, which are related to the negligible polarization discontinuity at the interfaces. Our results provide a deeper insight into the photoinduced properties in the 2D electron gas system, paving the way for the design of oxide optoelectronic devices.

Keywords: complex oxides, interface effect, photoconductivity

 Supplementary material for this article is available [online](#)

(Some figures may appear in colour only in the online journal)

1. Introduction

In recent years, striking discoveries have revealed that the two-dimensional electron gas (2DEG) confined at the oxide interfaces is a potential candidate for novel photonic and optoelectric devices [1, 2]. Particularly, the (001) LaAlO₃/SrTiO₃ (LAO/STO) heterointerfaces have been largely focused due to demonstrating a 2DEG with superconductivity, magnetic properties, electronic phase separation and so on [3–6]. Generally, the appearance of 2DEG at LAO/STO interfaces is ascribed to the electronic reconstruction induced by the polar discontinuity from the structural intrinsic nature [7, 8]. Therefore, the (111) LAO/STO interface, exhibiting the polar discontinuity, also has been confirmed to hold a 2DEG [9, 10]. These results strongly support this picture. Nevertheless, for the case of (110) LAO/STO heterointerfaces, STO can be represented by planar stacks of [SrTiO]⁴⁺ and [O₂]⁴⁻ and LAO can be represented by planar stacks of [LaAlO]⁴⁺ and [O₂]⁴⁻. Thus, there

are no polarization discontinuities at the interfaces. Based on the polar catastrophe, no 2DEG should be formed at (110) LAO/STO interfaces. However, recent experiments indicate that the unexpectedly high-mobility metallic conductivity has been observed at (110) LAO/STO interfaces [9, 11–13]. Therefore, the mechanism of 2DEG at the interface is still elusive [14–17]. On the other hand, light can be a powerful external perturbation that may be used to manipulate the transport properties [18–21]. In particular, the photoconductivity of 2DEG has attracted broad attention owing to the development of optoelectronic applications, such as optical switching devices and photo detectors [22, 23]. The persistent photoconductivity (PPC) with a large relaxation time has been observed at conductive LAO/STO (001) interfaces, indicating the role of band bending and vacancies [24]. Some effects of surface state, doping, electric field gating, on the photoconductivity, have also been investigated [25–27]. Until now, most of the researches are focused on photoresponsive properties of (001) LAO/STO heterointerfaces. And the investigation of photoresponsive properties at LAO/STO (111) and (110) interfaces

¹ Author to whom any correspondence should be addressed.

remains lack although it contributes to revealing intrinsic mechanisms of 2DEG. Thus, the photoresponsive properties of LAO/STO (111) and (110) interfaces are investigated by the illumination with a 360 nm light in this work.

2. Experimental techniques

Before the growth of LAO films by pulsed laser deposition, the STO ($5 \times 5 \times 0.5 \text{ mm}^3$) substrates were pretreated using different methods. For the (001) case, substrates were treated with well-established conditions: buffered HF for 41 s followed by thermal annealing at 970 °C for 2 h in air [28, 29]. For the (111)-oriented STO, the substrates were etched for 43 s and then annealed at 1000 °C for 2 h in air. For the (110)-oriented STO, the substrates were annealed for 150 min at 1000 °C in air without etching [30]. The surface of samples was examined by MFP-3D atomic force microscopy (AFM). All substrates show atomically smooth terraces and edges with steps corresponding to the STO interplanar distance in height as shown in figure S1 (stacks.iop.org/JPhysCM/32/135002/mmedia) in sup-info. The treated substrates were attached to a heater positioned 65 mm from the single crystalline LAO target. The growth parameters for the crystalline interfaces were as follows: 150 mJ/pulse for the laser energy, 800 °C for the deposition temperature, and different oxygen pressures (PO_2) ranging from 4×10^{-1} to 4×10^{-3} Pa. X-ray reflectivity (XRR) was carried out by a PANalytical X'Pert Pro x-ray diffractometer with $\text{Cu K}\alpha$ x-ray source. The thickness of LAO layer is estimated to be about 6.4 nm. The sheet resistance, carrier density, and carrier mobility were measured by using Van der Pauw method in a closed cycle He refrigerator with quartz glass windows. The four small contacts were placed on the corners of samples. Samples were irradiated using a light with a wavelength of 360 nm ($\sim 3.44 \text{ eV}$) and the power density was about 0.5 W cm^{-2} . The spot size of light was 4 mm in diameter after a beam expander and the light was focused uniformly on the area of films. The details of photoresponsive experiments were demonstrated in our recent works [31, 32].

3. Results

Figure 1(a)–(c) display AFM images, showing the surface morphology of the (001), (111), and (110) LAO/STO heterointerfaces deposited at 4×10^{-3} Pa, respectively. The terraces remain observable and there are no significant changes in the surface roughness as compared to STO substrates. The averaged surface roughness is about 105.1, 107.8 and 154.1 pm, respectively, indicating the uniform growth of LAO film.

The variations of sheet resistance, carrier density, and mobility as a function of temperature for (001), (111) and (110) LAO/STO heterointerfaces deposited at different PO_2 are shown in figures 2(a)–(c), respectively. As can be seen, the (110) sample shows a higher resistance than (001) and (111) LAO/STO interfaces deposited at the same PO_2 , suggesting the (001) and (111) interfaces produce better conductivity. This behavior is consistent with the normalized $R(T)$ curve with respect to its value at 300 K as given in figure S2

in sup-info. In addition, all the LAO/STO samples evidently exhibit a strong dependence on PO_2 of growth. Films deposited at 4×10^{-3} Pa present metallic interfaces as cooling from 300 K to 20 K. Increasing PO_2 to 4×10^{-2} Pa results in the presence of a distinct metal-to-insulator transition around $T = 30 \text{ K}$ upon cooling at the (110) LAO/STO heterointerface. However, the (001) and (111) LAO/STO heterointerfaces still maintain the metallicity. When PO_2 is increased to 4×10^{-1} Pa, all heterointerfaces favor the insulating behavior, which is similar to the observation at $\text{NdGaO}_3/\text{STO}$ interfaces related to oxygen vacancies in STO substrate [33–35]. For those heterointerfaces grown at a lower oxygen pressure, the high-density oxygen vacancies induce the larger carrier density [36, 37]. Carrier densities at different PO_2 further confirm this. The carrier densities vary from 3.7×10^{13} to $5.3 \times 10^{13} \text{ cm}^{-2}$, 3.5×10^{13} to $7.0 \times 10^{13} \text{ cm}^{-2}$, and 8.7×10^{13} to $14.7 \times 10^{13} \text{ cm}^{-2}$ at 300 K for (001), (111), (110) LAO/STO prepared at 4×10^{-2} and 4×10^{-3} Pa, respectively. It is obvious that the carrier densities of all the interfaces decrease during cooling below $\sim 100 \text{ K}$, suggesting the carrier freeze-out which can be ascribed to the carrier localization induced by oxygen vacancies as reported in STO [38]. In addition, it is also observed that the carrier mobilities of all the interfaces increase during cooling. For (001) and (111) LAO/STO interfaces, the mobilities at low temperature clearly increase with increasing PO_2 . However, for (110) LAO/STO interface, there is no significant change in mobility at different PO_2 .

To investigate the photoresponsive properties of (001), (111), and (110) LAO/STO heterointerfaces, we measure the time dependence of resistance for the heterointerfaces deposited at 4×10^{-2} Pa under a 360 nm light illumination at interval temperatures between 20 and 300 K, as shown in figure 3. The temporal dependence of resistance at heterointerfaces deposited at 4×10^{-3} and 4×10^{-1} Pa is displayed in sup-info (figures S3 and S4). It can be seen that all samples change from a high-resistance state to a low-resistance state when the light is on. The resistances of heterointerfaces under the irradiation decrease at different temperatures and cannot restore their originating values when the light is off. It is worthwhile to note that all the heterointerfaces show a PPC effect although the samples are fabricated on the substrates with different orientations.

In order to compare the change in resistance of samples induced by light, we define the photoinduced relative change in the resistance (ΔR_p) as $(R_d - R_p)/R_d$, where R_d is the resistance in dark and R_p is the resistance under light illumination [2]. The ΔR_p versus temperature curves for LAO/STO heterointerfaces deposited at different PO_2 are plotted in figure 4. It is obvious that the ΔR_p value is sensitive to the PO_2 as given in sup-info (figure S5) [39]. When $\text{PO}_2 = 4 \times 10^{-1}$ Pa, the ΔR_p value is nearly 100% at 20 K. However, it is about 90% at 20 K for the samples with $\text{PO}_2 = 4 \times 10^{-3}$ Pa. The value decreases monotonically with increasing temperature and gradually saturates as the temperature is above 100 K. In addition, it is obvious that (110) interfaces exhibit the lowest ΔR_p values in the temperature range of 20–300 K, which may be related to nonpolar discontinuity. On the contrary, the ΔR_p values of (001) and (111) interfaces are nearly the same at 4×10^{-2}

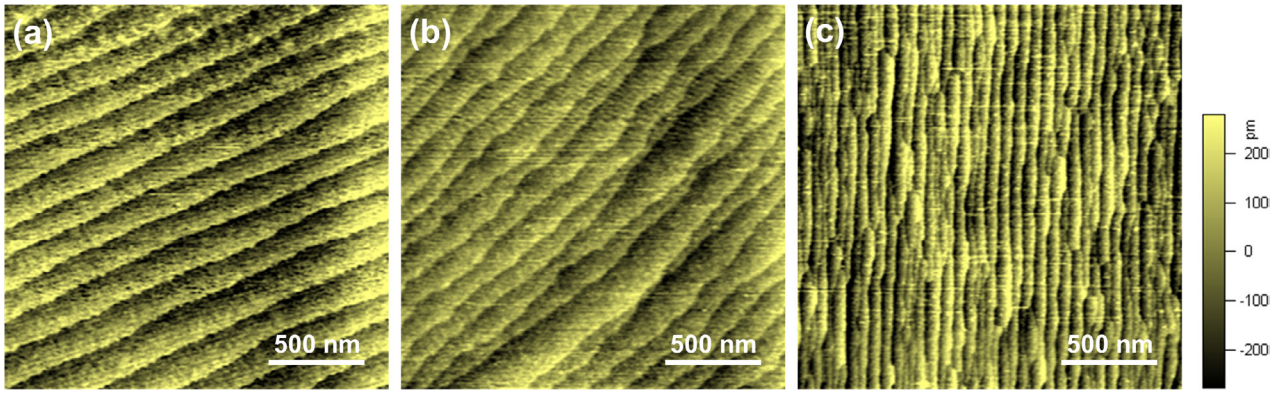


Figure 1. (a)–(c) The AFM images of LAO films deposited at $PO_2 = 4 \times 10^{-3}$ Pa on the (001), (111) and (110) STO substrates, respectively. The scale bar is 500 nm.

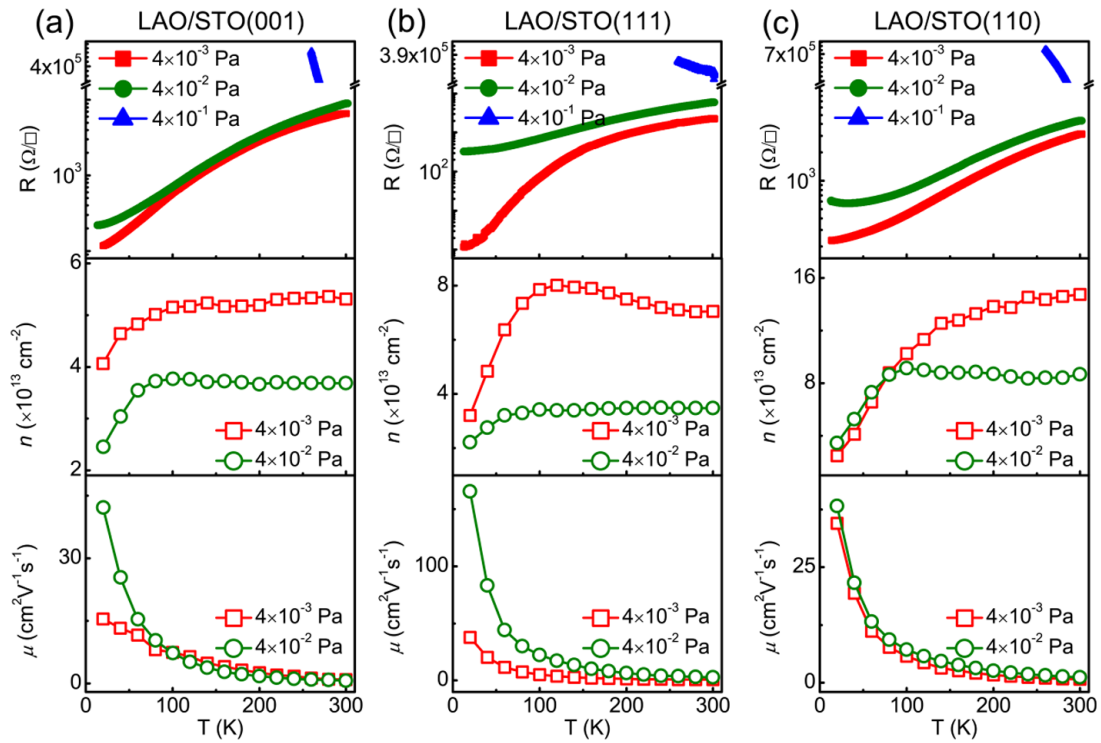


Figure 2. (a)–(c) Temperature dependence of sheet resistance, carrier density and electron mobility for (001), (111) and (110) LAO/STO heterointerfaces deposited at different PO_2 , respectively.

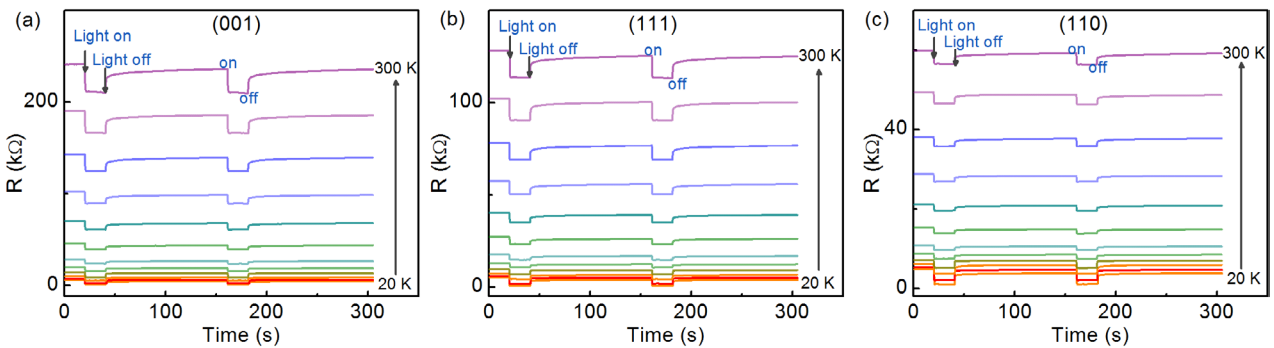


Figure 3. (a)–(c) Time evolution of resistance for (001), (111), and (110) LAO/STO heterointerfaces deposited at $PO_2 = 4 \times 10^{-2}$ Pa under the illumination at temperature range of 20 K–300 K, respectively.

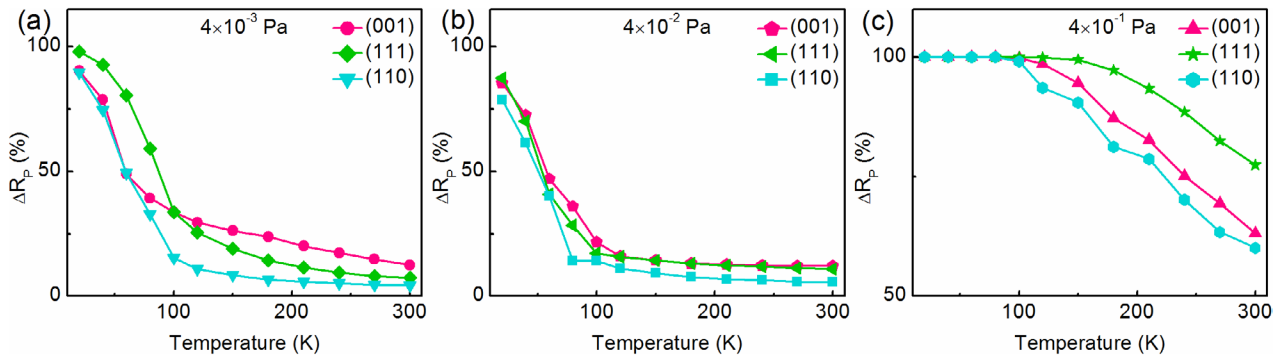


Figure 4. (a)–(c) Photoinduced change in the resistance as a function of temperature at (001), (111) and (110) LAO/STO heterointerfaces deposited at different PO_2 , respectively.

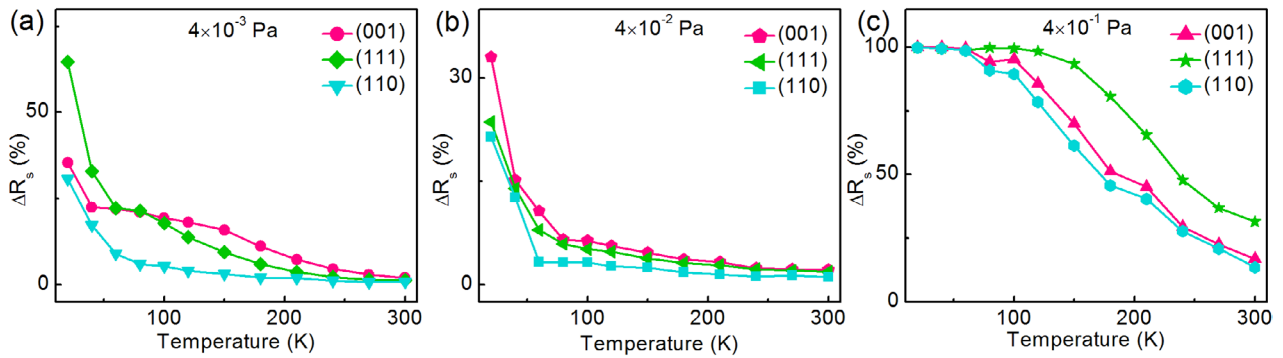


Figure 5. (a)–(c) Residual photoinduced change in the resistance as a function of temperature at (001), (111) and (110) LAO/STO heterointerfaces deposited at different PO_2 , respectively.

Pa. Besides this, it is also worth noting that the ΔR_p value of (111) interfaces is a little larger than (001) interfaces at low temperature at $PO_2 = 4 \times 10^{-3}$ Pa. This might be related with the larger lattice mismatch of (111) interfaces [9]. For further investigating the photoresponsive recovery process, we also concern on a surplus photoinduced change in the resistance (ΔR_s), which is defined as $(R_b - R_d)/R_d$, where R_b is the balanced resistance after the first illumination. Figure 5 shows the temperature dependence of ΔR_s . It is clearly that the ΔR_s value decreases with increasing the temperature. Besides, ΔR_s values increase with increasing PO_2 as given in sup-info (figure S6). It is also worth mentioning that the (110) interface exhibits the lowest ΔR_s values in the temperature range of 20–300 K, meaning the fastest recovery process.

4. Discussion

The change tendency of ΔR_p is caused by the thermal fluctuations at higher temperatures or the absence of lattice vibrations at low temperatures [40, 41]. The photon energy of light in the experiments is 3.44 eV (360 nm), which is higher than the band gap of STO. Hence, electrons are promoted from the valence band to the conduction band of STO close to the interface under irradiation. More electrons take part in the conduction, resulting in a decrease in the resistance in the metallic state of all the heterointerfaces. Moreover, because the oxygen vacancies locating inside the energy gap of STO also act as electron traps, PO_2 plays a significant role in the photoconductivity properties of LAO/STO interface. The samples deposited at

higher PO_2 with less oxygen vacancies exhibit larger ΔR_p [42, 43]. We can speculate that photogenerated carriers have a stronger effect on the heterointerfaces with lower carrier densities deposited at higher PO_2 .

It has been proved that oxygen vacancies at (001) LAO/STO act as electronic traps and locate below the conduction band of STO [44, 45]. Therefore, the photoexcited electrons will recombine immediately with the electron traps related to oxygen vacancies, when the light is off. Because less in-gap states will be formed with less oxygen vacancies, the slower recovery process is observed at the heterointerfaces fabricated in high PO_2 . Thus, the sample prepared in $PO_2 = 4 \times 10^{-1}$ Pa presents the slowest recovery process and hence the largest ΔR_s value. This is consistent with the fitting results of relaxation characteristics for the LAO/STO heterointerfaces grown at different PO_2 [39]. With the infrared ellipsometry and dc resistance measurements, Yazdi-Rizi *et al* found that a fraction of photogenerated charge carriers still persist after the light is switched off [46]. They obtained an evidence that the trapping of photogenerated oxygen vacancies at defects would strongly influence the lifetime of related itinerant electrons. Their results also point out the main difference between (001) LAO/STO and (110) LAO/STO heterostructures. For the former interfaces, the permanent charge carriers are likely caused by polar catastrophe or the fully saturated and stable oxygen vacancies in initial state (polar catastrophe also play important role in this case). But for (110) LAO/STO heterostructures, the carriers that are trapped in the vicinity of interfaces originating from oxygen vacancies. Therefore, the results show that oxygen vacancies play a crucial role in

the photoresponsive properties of (001), (111) and (110) LAO/STO heterointerfaces. More importantly, the difference among three interfaces in photoresponse also deserves special attention. For (001) and (111) interfaces, both polar discontinuity and oxygen vacancies jointly contribute to the interfacial conduction. However, only oxygen vacancies are responsible for the conductivity at the (110) interface. This is the reason that the photoresponsive properties of (001) and (111) LAO/STO interfaces are stronger than that of (110) LAO/STO.

5. Conclusions

In conclusion, we have carried out a comprehensive photoresponsive study of (001), (111), and (110) LAO/STO heterointerfaces deposited at different oxygen pressures. It is obtained that the polar discontinuity is responsible for the differences in photoresponse between (001), (111), and (110) LAO/STO heterointerfaces. In addition to this, the photoinduced resistance modulation of LAO/STO heterointerface is highly sensitive to the oxygen vacancies. The heterointerfaces with less oxygen vacancies exhibit a larger resistance change when illuminated by light and a slower recovery process when light is turned off. These results are significant for studying the properties of oxide 2DEG.

Acknowledgments

This work was supported by the National Natural Science Foundation of China (nos. 51572222, 11604265, and 61471301) and sponsored by Innovation Foundation for Doctor Dissertation of Northwestern Polytechnical University (no. CX201836).

ORCID iDs

Hong Yan  <https://orcid.org/0000-0003-1146-679X>
 Zhaoting Zhang  <https://orcid.org/0000-0002-0791-9904>
 Ming Li  <https://orcid.org/0000-0002-2469-6706>
 Shuanhu Wang  <https://orcid.org/0000-0002-5386-1037>
 Lixia Ren  <https://orcid.org/0000-0002-1191-6087>
 Kexin Jin  <https://orcid.org/0000-0001-5838-0315>

References

- [1] Jin K X, Lin W, Luo B C and Wu T 2015 *Sci. Rep.* **5** 8778
- [2] Yan H, Zhang Z T, Wang S H, Ren L X, Li M, Chen C L and Jin K X 2019 *J. Mater. Sci.* **54** 108
- [3] Ohtomo A and Hwang H Y 2004 *Nature* **427** 423
- [4] Reyren N *et al* 2007 *Science* **317** 1196
- [5] Dikin D A, Mehta M, Bark C W, Folkman C M, Eom C B and Chandrasekhar V 2011 *Phys. Rev. Lett.* **107** 056802
- [6] Bert J A, Kalisky B, Bell C, Kim M, Hikita Y, Hwang H Y and Moler K A 2011 *Nat. Phys.* **7** 767
- [7] Savoia A *et al* 2009 *Phys. Rev. B* **80** 075110
- [8] Nakagawa N, Hwang H Y and Muller D A 2006 *Nat. Mater.* **5** 204
- [9] Herranz G, Sánchez F, Dix N, Scigaj M and Fontcuberta J 2012 *Sci. Rep.* **2** 758
- [10] Davis S K, Huang Z, Han K, Ariando X X, Venkatesan T and Chandrasekhar V 2017 *Adv. Mater. Interfaces* **4** 1600830
- [11] Annadi A *et al* 2013 *Nat. Commun.* **4** 1838
- [12] Gopinadhan K, Annadi A, Kim Y, Srivastava A, Kumar B, Chen J S, Coey J, Michael D, Ariando X X and Venkatesan T 2015 *Adv. Electron. Mater.* **1** 1500114
- [13] Han Y L *et al* 2015 *Phys. Rev. B* **92** 115304
- [14] Chen Y Z, Pryds N, Kleibeuker J E, Koster G, Sun J R, Stamate E, Shen B G, Rijnders G and Linderöth S 2011 *Nano Lett.* **11** 3774
- [15] Chambers S A *et al* 2010 *Surf. Sci. Rep.* **65** 317
- [16] Li M, Yan H, Zhang Z T, Ren L X, Zhao J, Wang S H, Chen C L and Jin K X 2018 *J. Appl. Phys.* **124** 145301
- [17] Segal Y, Ngai J H, Reiner J W, Walker F J and Ahn C H 2009 *Phys. Rev. B* **80** 241107
- [18] Zhang Z T, Yan H, Wang S H, Wang M, Ren L X, Chen C L and Jin K X 2019 *J. Mater. Sci.* **54** 4780
- [19] Jin K X, Yang B, Zhang Y, Luo B C, Chen L Y and Chen C L 2016 *Scr. Mater.* **112** 62
- [20] Jin K X, Zhao S G, Tan X Y and Chen C L 2008 *J. Phys. D: Appl. Phys.* **41** 045105
- [21] Zhang Z T, Yan H, Wang S H, Ren L X, Chen C L and Jin K X 2018 *Scr. Mater.* **156** 64
- [22] Tebano A, Fabbri E, Pergolesi D, Balestrino G and Traversa E 2012 *ACS Nano* **6** 1278
- [23] Liang H X *et al* 2013 *Sci. Rep.* **3** 1975
- [24] Di Gennaro E *et al* 2013 *Adv. Opt. Mater.* **1** 834
- [25] Chan N Y, Zhao M, Wang N, Au K, Wang J, Chan L, Wa H and Dai J Y 2013 *ACS Nano* **7** 8673
- [26] Yan H, Zhang Z T, Wang S H, Zhang H R, Chen C L and Jin K X 2017 *ACS Appl. Mater. Interfaces* **9** 39011
- [27] Lei Y *et al* 2014 *Nat. Commun.* **5** 5554
- [28] Kawasaki M, Takahashi K, Maeda T, Tsuchiya R, Shinohara M, Ishiyama O, Yonezawa T, Yoshimoto M and Koinuma H 1994 *Science* **266** 1540
- [29] Koster G, Kropman B L, Rijnders G J H M, Blank D H A and Rogalla H 1998 *Appl. Phys. Lett.* **73** 2920
- [30] Biswas A, Rossen P B, Yang C H, Siemons W, Jung M H, Yang I K, Ramesh R and Jeong Y H 2011 *Appl. Phys. Lett.* **98** 051904
- [31] Yan H, Zhang Z T, Wang S H, Wei X Y, Chen C L and Jin K X 2018 *ACS Appl. Mater. Interfaces* **10** 14209
- [32] Yan H, Wang S H, Zhang Z T, Zhang H R, Chen C L and Jin K X 2018 *J. Appl. Phys.* **124** 035302
- [33] Li C, Xu Q F, Wen Z, Zhang S T, Li A D and Wu D 2013 *Appl. Phys. Lett.* **103** 201602
- [34] Brinkman A, Huijben M, Van Zalk M, Huijben J, Zeitler U, Maan J C, Van der Wiel W G, Rijnders G, Blank D H A and Hilgenkamp H 2007 *Nat. Mater.* **6** 493
- [35] Chen Y Z, Christensen D V, Trier F, Pryds N, Smith A and Linderöth S 2012 *Appl. Surf. Sci.* **258** 9242
- [36] Santander-Syro A F *et al* 2011 *Nature* **469** 189
- [37] Schwingenschlögl U and Schuster C 2009 *Chem. Phys. Lett.* **467** 354
- [38] Liu Z Q *et al* 2013 *Phys. Rev. X* **3** 021010
- [39] Liu G Z, Qiu J, Jiang Y C, Zhao R and Gao J 2018 *Mater. Res. Express* **5** 046308
- [40] Li M Y, Graf T, Schladt T D, Jiang X and Parkin S S P 2012 *Phys. Rev. Lett.* **109** 196803
- [41] Jin K X, Zhao S G, Tan X Y, Chen C L and Jia X W 2009 *Appl. Phys. A* **95** 789
- [42] Liu Z Q *et al* 2011 *Phys. Rev. Lett.* **107** 146802
- [43] Liu G Z, Qiu J, Jiang Y C, Zhao R, Yao J L, Zhao M, Feng Y and Gao J 2016 *Appl. Phys. Lett.* **109** 031110
- [44] Kalabukhov A, Gunnarsson R, Börjesson J, Olsson E, Claesson T and Winkler D 2007 *Phys. Rev. B* **75** 121404
- [45] Wang X, Chen J Q, Roy Barman A, Dhar S, Xu Q H, Venkatesan T and Ariando X X 2011 *Appl. Phys. Lett.* **98** 081916
- [46] Yazdi-Rizi M, Marsik P, Mallett B P P, Sen K, Cerreta A, Dubroka A, Scigaj M, Sánchez F, Herranz G and Bernhard C 2017 *Phys. Rev. B* **95** 195107